SANDIA REPORT
SAND2012-6745
Unlimited Release
Printed August 2012

PV Power Output Smoothing using Energy Storage

Abraham Ellis and David Schoenwald
Sandia National Laboratories

Jon Hawkins, Steve Willard, and Brian Arellano
Public Service Company of New Mexico

Prepared by
Sandia National Laboratories
Albuquerque, New Mexico 87185 and Livermore, California 94550

Sandia National Laboratories is a multi-program laboratory managed and operated by Sandia Corporation, a wholly owned subsidiary of Lockheed Martin Corporation, for the U.S. Department of Energy's National Nuclear Security Administration under contract DE-AC04-94AL85000.

Approved for public release; further dissemination unlimited.

Sandia National Laboratories

Issued by Sandia National Laboratories, operated for the United States Department of Energy by Sandia Corporation.

NOTICE: This report was prepared as an account of work sponsored by an agency of the United States Government. Neither the United States Government, nor any agency thereof, nor any of their employees, nor any of their contractors, subcontractors, or their employees, make any warranty, express or implied, or assume any legal liability or responsibility for the accuracy, completeness, or usefulness of any information, apparatus, product, or process disclosed, or represent that its use would not infringe privately owned rights. Reference herein to any specific commercial product, process, or service by trade name, trademark, manufacturer, or otherwise, does not necessarily constitute or imply its endorsement, recommendation, or favoring by the United States Government, any agency thereof, or any of their contractors or subcontractors. The views and opinions expressed herein do not necessarily state or reflect those of the United States Government, any agency thereof, or any of their contractors.

Printed in the United States of America. This report has been reproduced directly from the best available copy.

Available to DOE and DOE contractors from
U.S. Department of Energy
Office of Scientific and Technical Information
P.O. Box 62
Oak Ridge, TN 37831

Telephone: (865) 576-8401
Facsimile: (865) 576-5728
E-Mail: reports@adonis.osti.gov
Online ordering: http://www.osti.gov/bridge

Available to the public from
U.S. Department of Commerce
National Technical Information Service
5285 Port Royal Rd.
Springfield, VA 22161

Telephone: (800) 553-6847
Facsimile: (703) 605-6900
E-Mail: orders@ntis.fedworld.gov
Online order: http://www.ntis.gov/help/ordermethods.asp?loc=7-4-0#online

SAND2012-6745
Unlimited Release
Printed August 2012

PV Power Output Smoothing using Energy Storage

Abraham Ellis and David Schoenwald
Sandia National Laboratories
P.O. Box 5800
Albuquerque, New Mexico 87185-MS1033

Jon Hawkins, Steve Willard, and Brian Arellano
Public Service Company of New Mexico
414 Silver Avenue SW
Albuquerque, NM 87102-3289

Abstract

This paper describes a simple algorithm designed to reduce the variability of photovoltaic (PV) power output by using an energy storage device. A full-scale implementation was deployed in an actual PV Energy demonstration project, in partnership with a utility and a battery manufacturer. The paper describes simulation tests as well as field results. In addition to demonstrating implementation of smoothing controls, this work also served to verify the models, identify best parameter sets for utility operations, and study the operation of an advanced energy storage system under partial state of charge and rapid, irregular charge/discharge cycling.

ACKNOWLEDGMENTS

The demonstration project is being conducted with support from DOE Smart Grid Demonstration Grant in Energy Storage (DE-OE-0000230), a collaborative effort that involves PNM, EPRI, East Penn Manufacturing Co., Northern New Mexico College, Sandia National Laboratories and the University of New Mexico. A portion of this work was supported by the US Department of Energy Solar Energy Technologies Program.

CONTENTS

1. INTRODUCTION 7
2. PV AND BATTERY SYSTEM MODELING 8
3. DESCRIPTION OF SMOOTHING AND SOC TRACKING ALGORITHM 11
4. PERFORMANCE TESTING AND PARAMETER TUNING 12
   4.1. Test Cases 1-3 12
   4.2. Other Tests 16
5. FIELD IMPLEMENTATION 17
6. CONCLUSION 19
7. REFERENCES 20
DISTRIBUTION 21

FIGURES

Fig 1. Diagram of PV smoothing algorithm. 9
Fig 2. Power plots for Test Case #1 13
Fig 3. SOC plots for Test Case #1 13
Fig 4. Power plots for Test Case #2 14
Fig 5. SOC plots for Test Case #2 14
Fig 6. Power plots for Test Case #3 15
Fig 7. SOC plots for Test Case #3 15
Fig 8. Power plots from demonstration site for a representative day 17
Fig 9. Detail of the dashed area in Fig. 8 18

TABLES

Table 1. Parameters for PV Smoothing Algorithm 8

NOMENCLATURE

ACE	Area Control Error
BESS	Battery Energy Storage System
DB	Dead Band
DOE	Department of Energy
IT	Information Technology
kV	kilo Volts
kW	kilo Watts
kWh	kilo Watt-hours
LPF	Low Pass Filter
MA	Moving Average
MAX	Maximum
MIN	Minimum
PCS	Power Conditioning System
PV	Photovoltaic
REF	Reference
SCADA	Supervisory Control and Data Acquisition
SNL	Sandia National Laboratories
SOC	State of Charge

1. INTRODUCTION

This paper describes an algorithm designed to reduce the variability of photovoltaic (PV) power output by using a battery. The purpose of the battery is to add power to the PV output (or subtract power from the PV output) to smooth out the high frequency components of the PV power that occur during periods with transient cloud shadows on the PV array. The control system is challenged with the task of reducing short-term PV output variability while avoiding the overworking of the battery, both in terms of capacity and ramp capability. The algorithm proposed in this paper is purposely very simple to facilitate implementation in a real-time controller. A separate battery energy storage system (BESS) commands the battery power level based on a power reference computed by the smoothing algorithm. The smoothing algorithm can be configured to compute the reference signal that the control system is trying to track, either a moving average (MA) of the PV power, or the PV power processed through a low pass filter (LPF). The purpose of the control system then is to balance the tasks of tracking the reference state of charge (SOC) value with the desired smoothing function. To improve the robustness of the control system to battery parameters and time delays, a dead band function was added to the battery control system. The dead band function will prevent the battery from tracking small excursions from the baseline smoothing function, deemed to be too small to warrant control action. The control structure has two additional inputs to which the battery can respond. For example, the battery could respond to PV variability, load variability or area control error (ACE) or a combination of the three. This algorithm has been implemented in a field study described in [1], [2], and [3]. The PV-battery demonstration system consists of a 500 kW PV system with two ac-coupled batteries. One of the battery banks is a conventional lead-acid battery with 1 MWh of capacity and dedicated 250 kW power electronics interface, and is used for energy shifting. The second battery is a "power battery" designed with 1000 kW-h of capacity and dedicated 500 kW power electronics interface. This battery was designed for long cycle life at partial state of charge and high charge/discharge rates. The algorithm described in this paper only manages the operation of the smoothing battery.

The concept of smoothing for renewable energy generation has been studied in the literature (see [4]-[6]). This paper looks at implementation issues for an actual utility scale experiment. The paper is organized as follows: Section 2 describes the algorithm development, starting with a simple simulation in Matlab. Section 3 describes the algorithm in more detail. Section 4 describes some of the test cases and parameter tuning. Concluding remarks and field tests results are offered in Section 5.

2. PV AND BATTERY SYSTEM MODELING

For the purposes of control design and testing, the battery was modeled as a simple kW-hour accumulator (integrator). Detailed representation temperature effects, efficiency and terminal voltage characteristics is not strictly required to demonstrate smoothing control. The battery energy storage system (BESS) continuously computes the state of charge (SOC) of the battery and makes it available to the smoothing control. The BESS also enforces limits on the maximum charge and discharge ramp rate, as well as the range of state of charge (SOC) within which the battery is allowed to operate. In the model, the SOC limits enforced by the BESS are simply represented as non-windup saturation limits on the integrator. For the purposes of control design, the usable battery SOC range is defined to be 40% to 80% of the battery size (1000 kW-h in this specific case). This is a range where efficiency is very high and impact on life expectancy is quite acceptable for the particular battery technology being used. The SOC limits are expressed as fractions (0.4 and 0.8 in this case). The smoothing algorithm allows for explicit representation of ramp limits. The PV/battery demonstration system is designed such that the charge/discharge rate of the smoothing battery is only limited by the size of the power electronics interface; therefore, there was no need to explicitly limit ramp rate limits in the algorithm. The outline of the algorithm appears in Fig. 1 with the default parameters in Table 1.

Table 1. Parameters for PV Smoothing Algorithm

PARM.	NAME	UNITS	DEFAULT VALUE
T_W	PV Moving Average Time Window	seconds	3600 (1 hour)
T_1	PV Low Pass Filter Time Constant	seconds	3600 (1 hour)
T_2	AUX1 (load) Low Pass Filter Time Constant	seconds	3600 (1 hour)
T_3	AUX2 (ACE) Low Pass Filter Time Constant	seconds	0
Flag	Switch between LPF and MA	0 or 1, 0=use MA, 1=use LPF	1 (use LPF)
G_1	PV Smoothing Error Gain	unit less	1 (for 100% compensation)
G_2	AUX1 (load) Scaling Factor	unit less	depends on magnitude of AUX1 signal
G_3	AUX2 (ACE) Scaling Factor	unit less	Depends on magnitude of AUX2 signal
G_4	SOC Tracking Gain	unit less	1000
DB	Dead Band Width	kW	+/- 50
SOC_{REF}	Reference State of Charge	unit less (within defined SOC limits)	0.6

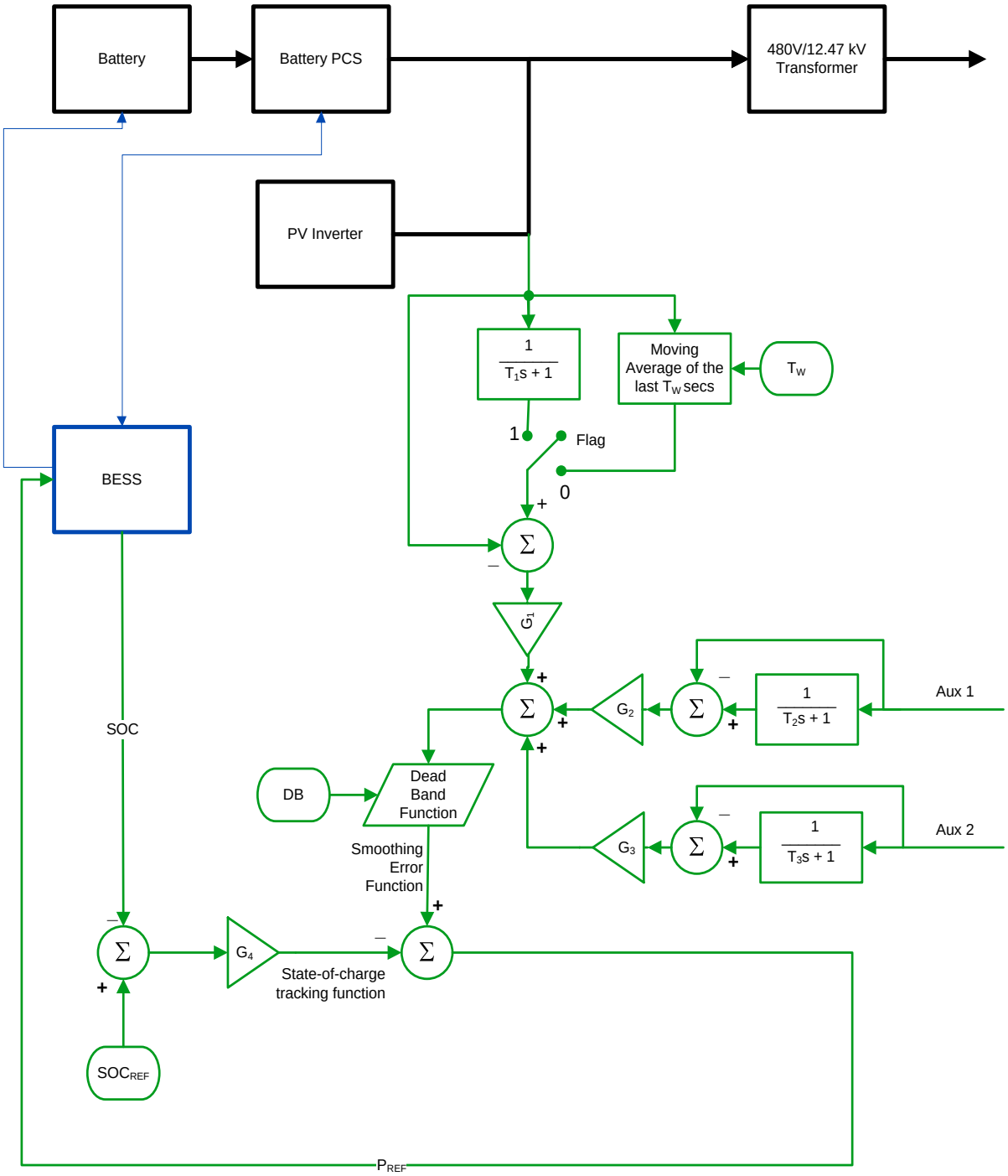

Fig 1. Diagram of PV smoothing algorithm.

The initial condition of the accumulator is set to the desired reference SOC value within the allowable range. For this application, a point in the middle of the range was selected which is 0.6 (60% SOC). A time delay was used as a simple way to represent the response time of the BESS and controls in the power electronic devices. The delay is represented by a time constant T_{BESS}. In this specific application, it is assumed that the delay is on the order of 1 sec. Considering that the output of a large PV system over one second is relatively small (certainly

compared to changes on irradiance measured by a pyranometer) due to the PV array footprint, the time delay introduced by the BESS controls is not large enough to require the use of more complex controls such as predictive or adaptive methods. The power rating of the power electronics are modeled with a simple power limiter, set to +/- 500 kW, in this particular case. For testing purposes, the PV system was modeled simply as a power injection. Output data from an actual 500 kW PV system in a similar climate region was used to test the smoothing algorithm and adjust parameters. Note that, because the algorithm is implemented in Simulink in discrete time using a time step of one second, the power signal going into the integrator is scaled by a factor of 1/3600, which translates power into units of kW-hour. This scaling factor was explicitly included so that it can be in the real-time controller based on control sampling rate and bandwidth.

In summary, the battery energy storage system ultimately commands the battery power level based on a power reference computed by the smoothing algorithm. The BESS takes the desired battery power computed by the smoothing algorithm and updates the battery reference power. The battery is assumed to respond with a time constant of TBESS. A saturation function is applied to limit the requested battery power to no more than +/- the power electronics size (500 kW in this example). Finally, we represent SOC_{MAX} SOC_{MIN} limits imposed by the BESS using a simple non-windup saturation model. The default parameters in Table 1 were derived assuming a control system sampling rate of 1 second, and for the specific application considered during testing.

3. DESCRIPTION OF SMOOTHING AND SOC TRACKING ALGORITHM

The smoothed reference signal that the control system is trying to track is either a time moving average (MA) of the PV power, or the PV power processed through a low pass filter (LPF). One of the editable parameters is a flag that determines which of these two smoothing functions is selected. A flag value of 1 implies that the LPF is chosen and a flag value of 0 implies that the MA is chosen. Each of these smoothing functions has a single user editable parameter. The MA function uses the length of the time window, T_W in secs, for its parameter. The default value is 3600 secs (one hour). The LPF function uses the time constant, T_1 also in secs, for its parameter. Again, the default value is 3600 secs. If T_W and T_1 are the same, the two methods create roughly the same smooth reference signal. Fig. 1 shows that it is possible to include two auxiliary signals (AUX1 and AUX2) as part of the smoothing function. Both of these can be low pass filtered as well. In general, this control structure allows for representation of a smoothing function of the form G_1 x E_1 + G_2 x E_2 + G_3 x E_3, where E1 is the PV smoothing error signal, E_2 and E_3 are filtered error signals based on AUX1 and AUX2 inputs, and G_1, G_2, G_3 are scaling factors. Neither of the two AUX signals was used in testing of the algorithm, but placeholders exist in the model (and controller) for both. After the smoothing function is obtained, it may be desirable to apply a dead band function to prevent the battery from tracking small excursions from the baseline smoothing function. This dead band width is user settable. For this example, a dead band width of +/- 50 kW was chosen. Table 1 gives the default values for these parameters.

The purpose of the control system is to balance the tasks of tracking the reference SOC value (0.6 in this example) with the desired smoothing function. The state of charge tracking error (difference between the reference SOC and the actual SOC) is multiplied by a proportional gain, G_4, to produce the state of charge tracking signal. The gain represents how aggressively the battery is returned to the reference state of charge. In a practical application, the gain should be set small enough to allow the smoothing function to take precedence, but large enough to prevent the battery from continuously reaching the defined SOC limits. The SOC tracking signal is then subtracted from the desired smoothing function to determine the reference (requested) battery power for that time step. Once the control system determines the requested battery power this is sent to the BESS which implements it as described above. It should be pointed out that, assuming that the two auxiliary signals are not being used, the two primary parameters of interest are T_W (or T_1 if the LPF is being used) and G_4. When G_1 is set to 1.0, the battery would be commanded to compensate for 100% of the difference between actual PV output and the smooth reference. A value smaller than 1.0 can be used if the battery capacity or the power electronics rating is small with respect to the expected PV power error signal. As one increases the time window (or LPF time constant) the smoothed reference signal becomes smoother with slower ramps. The tradeoff is that the battery must make up a larger difference on average for every time step, hence the SOC will have larger excursions from the SOC reference value. Conversely, as G4 is increased, more emphasis is placed on close tracking of the SOC reference value at the expense of a smoother injected power. The tradeoff between these two parameters allows one to tune the control system to an acceptable balance between the two tasks. Note that the dead band width can also be part of this tuning process.

4. PERFORMANCE TESTING AND PARAMETER TUNING

Various scenarios of parameter values were simulated to illustrate the behavior of the smoothing algorithm and to select appropriate default parameters for the intended application[1]. For the performance testing, the PV power output was taken from a one day (86400 seconds) profile of measured output from an actual 500 kW PV plant in the southwest US. The selected sample day exhibits significant power output dynamics with some high ramping events, due to cloud shadows on the PV array. Simulations were conducted on 2-5 day PV input signals with very similar results. In all cases, the sampling rate of the control system was assumed to be 1 second, for simplicity. System assumptions are as follows:

- 500 kW PV system
- 1000 kWh battery storage
- 500 kW energy storage power electronics converter
- 0.4 to 0.8 SOC usable range for smoothing
- SOC reference value of 0.6

Further, the flag was set to zero meaning that the moving average smoothing algorithm was always used. The low pass filter (LPF) was simulated as well with very similar results. The LPF did result in a slightly smoother tracking function, but the difference is not significant. The PV smoothing gain, G_1, was set to 1.0 in all test cases. Neither of the auxiliary signals were used during these tests, and thus G_2=G_3=0 in all cases. For these test cases, the deadband function was disabled (DB = 0.0 kW).

In each case two plot charts are presented. The first chart consists of 5 plots of power vs. time where power is in kW and time is in seconds. The first plot is that of PV power. The second plot represents the desired smoothed output. The third plot corresponds to the actual power injected to the grid, which is the sum of PV power plus battery power. The fourth plot represents the difference (in kW) between the actual injected power and the desired smoothed output. The fifth plot corresponds to the power that the battery actually delivers (positive means the battery added to the injected power and negative means the battery used the power to increase its SOC). The difference reflects the battery system response time and SOC limitations, as described in the PV and Battery System Modeling section. The second chart consists of 2 plots of SOC vs. time (in seconds). The first plot is that of the SOC tracking function which is an error tracking signal that is scaled by G4 and has the units of kW. The second plot corresponds to the actual SOC which is a fraction that should always be between 0.4 and 0.8 (desired value is 0.6 in every case). The results of the test cases discussed below are shown in Figs. 2-7.

4.1. Test Cases 1-3

Test Case #1 simulates a 15 minute moving average (TW=900 seconds) for the smoothing function with a nominal SOC tracking gain (G_4=1,000). Fig. 2 shows the simulation results for the key input, output and control signals. From top to bottom, these signals are: (a) PV system output (kW) (b) desired PV plus battery output after smoothing (kW); (c) actual net power

[1]The default parameters will be tuned based on local solar resource characteristics, specific control objectives, and observed system performance.

injected to the grid (kW); (d) smoothing battery state of charge (per unit); and (e) battery power (kW). Note that the injected power tracks the smoothing function very well with an error not exceeding 28 kW at any time throughout the day. Since the battery is capable to charge and discharge at a rate higher than weather-driven PV output power changes, the observed discrepancy is due to the BESS control delay and the effect of SOC tracking. A higher discrepancy would be observed when the battery reaches a SOC limit, or the deadband is set to a large value. The battery power delivered only briefly exceeds +/- 200 kW. Fig. 3 illustrates that the battery SOC remains in a tight range about the reference SOC barely deviating more than +/- 0.02 per unit (2%) from the reference SOC throughout the day. This shows that the battery is able to achieve a 15-minute smoothing average by utilizing only a fraction of its defined usable capacity of 40% (0.4 to 0.8 SOC).

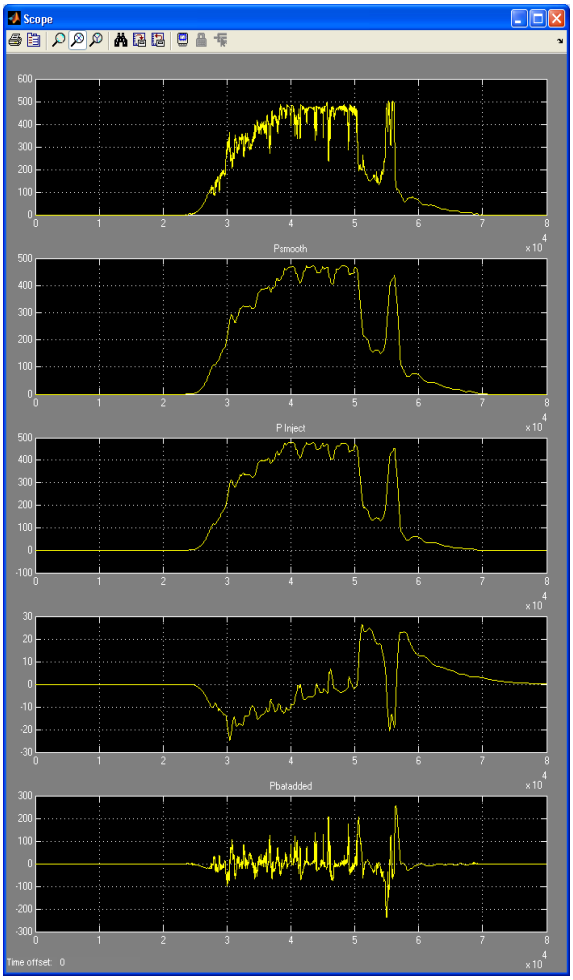

Fig 2. Power plots for Test Case #1

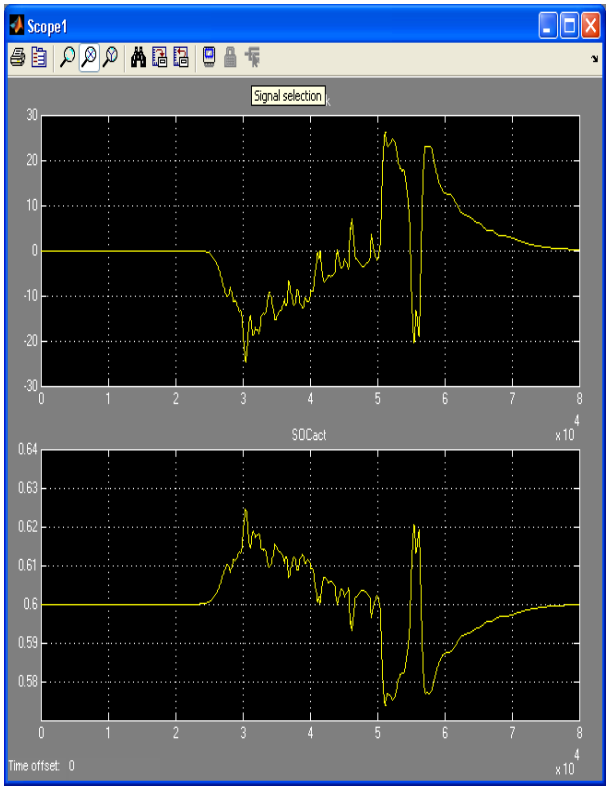

Fig 3. SOC plots for Test Case #1

Test Case #2 is identical to Test Case #1 except that the SOC tracking gain is increased by a factor of 10 (G4=10,000). The purpose of this case is to show how tighter tracking of the SOC reference value (i.e. higher G4 value) affects the tracking of the smoothing function. Fig. 4 shows that the smoothing error increases significantly resulting in more high frequency components in the injected power signal. The tradeoff is illustrated in Fig. 5 which shows that the battery SOC deviates only about half as much as in Test Case #1. But since the SOC was

already well regulated in the first test case, the tradeoff in increased smoothing error is likely not worth the improvement in SOC tracking.

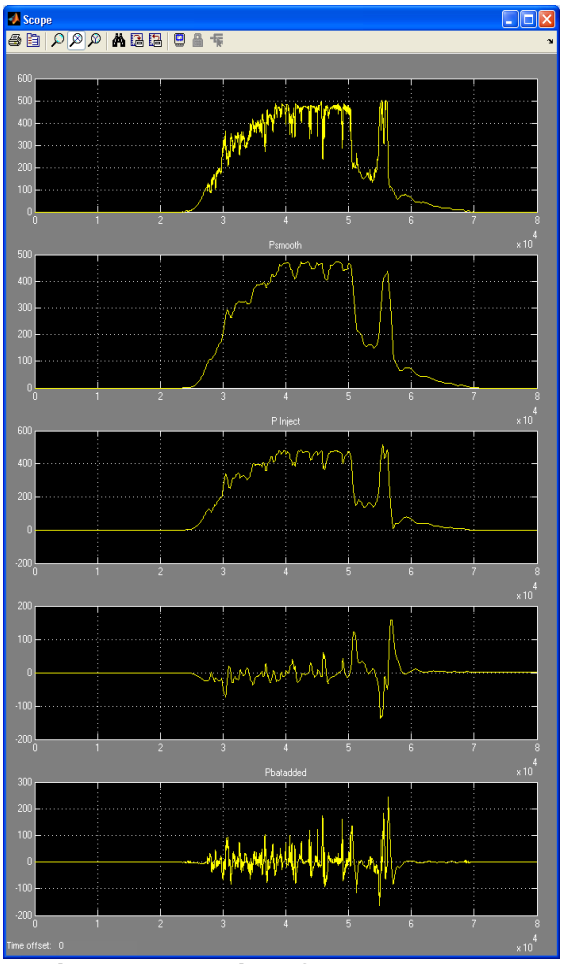

Fig 4. Power plots for Test Case #2

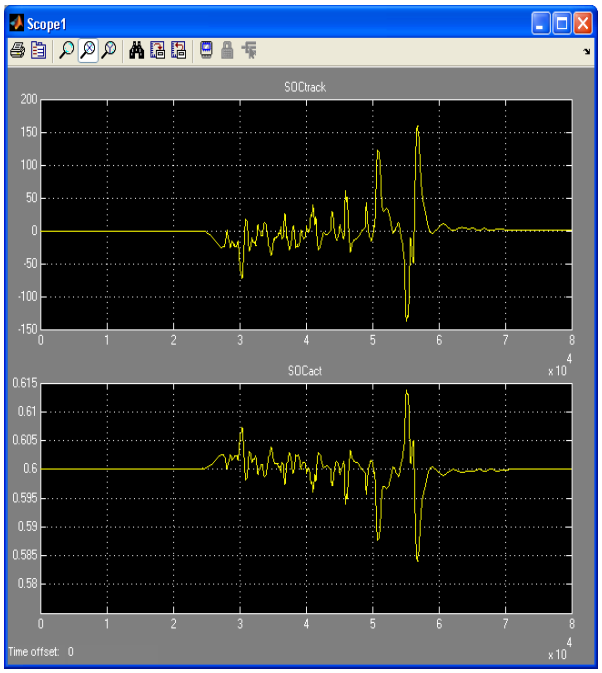

Fig 5. SOC plots for Test Case #2

The only change in Test Case #3 is to reduce the SOC tracking gain by a factor of 10 from the nominal value (e.g. G4=100). Fig. 6 shows the best smoothing function tracking performance of the first 3 test cases with smoothing errors of no more than +/- 4 kW. The price paid is shown in Fig. 7 with the battery SOC deviating a little more than in the prior test cases, though not by a significant amount. Test cases 1-3 taken together show that a nominal value of G_4=1,000 is quite reasonable with significantly lower values not necessarily stressing the battery that much more while providing improved smoothing performance. Note that for smaller battery sizes, higher deviations from the reference SOC value may not be tolerable, thus the tradeoff between smoothing and SOC tracking is more significant, and thus the value of G4 should be chosen carefully.

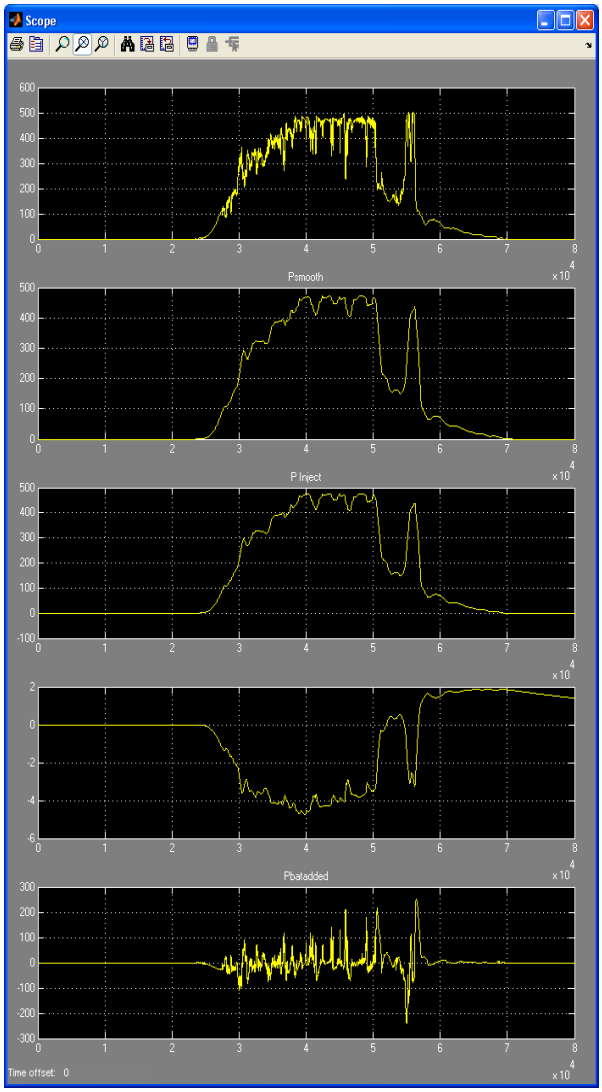

Fig 6. Power plots for Test Case #3

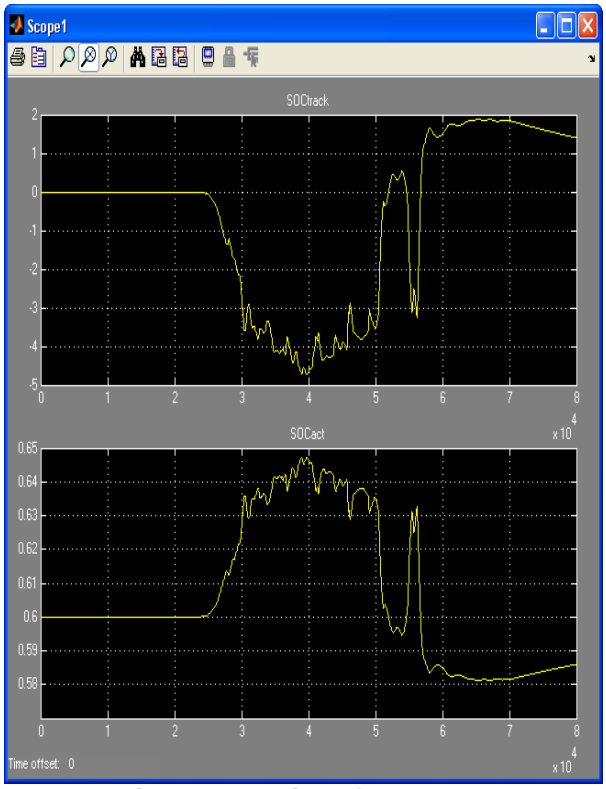

Fig 7. SOC plots for Test Case #3

4.2. Other Tests

Further testing was conducted with longer average time window, as high as 2 hours. For these tests, SOC remains well within the 0.4 to 0.8 limits, and the required battery power rarely challenges the rating of the power electronics. Of course, longer time windows improve the smoothing performance at the expense of increasing the battery usage and higher charge/discharge rates. In the interest of brevity, however, further results are not shown. The use of the low pass filter instead of the moving average showed a small improvement in smoothing performance with minimal additional battery usage. The simulation of all these tests resulted in the nominal parameter values chosen in Table 1 which produced a reasonable overall performance.

For smaller battery sizes, even small deviations from the reference SOC value may not be tolerable, thus the tradeoff between smoothing and SOC tracking can be significant. Hence, the value of G_4 should be chosen carefully. Further tests were conducted with the dead band ranging between 0 and 50 kW. The results of these tests showed that total energy conditioned by the battery can be reduced with nonzero dead band values while maintaining good smoothing characteristics.

5. FIELD IMPLEMENTATION

The PV smoothing controls described in this paper have been implemented in a full-scale PV-battery demonstration project. As described in Section 1, the energy storage system consists of two different batteries, one designed for energy and the other designed for power smoothing. The smoothing and shifting controls are coordinated to eliminate undesirable interaction. For example, the smoothing battery dies not react to dispatch of the shifting battery. As part of the demonstration project, the host utility is performing a variety of tests to determine optimum parameters to support operations. Operators are able to change control parameters remotely, via SCADA system. In practice, SOC limits have been set at 0.3 to 0.7. Field experiments conducted this far have been done with the moving average function. The smoothing time constant is 900 seconds. A dead band of 50 kW was considered acceptable to balance smoothing performance and battery effort. The maximum ramp rates observed at the site are on the order of 130 kW/sec, which is well below the maximum battery charge/discharge rate. Much of the experimentation has been around settings of the parameter G_1 (smoothing control gain), which affects the rate of response of the battery. Operation of the system has been as expected, and field results have served to validate the simple model approach described in Section 2.

As an example, Figs. 8 and 9 illustrate the performance of the smoothing algorithm for a typical PV input profile. For this experiment, parameters chosen were $T_W = 900$ seconds, $G_1 = 1$, $G_4 = 1{,}000$, and a dead band of 50 kW. Note that the battery (blue trace) counter-acts the fast changes in PV power (red trace). The combined output (green trace) is variable, but with a ramp rate appreciably smaller than the PV power. This experimental case compares well to the simulation Test Case #1 with the addition of a dead band. Fig. 8 also shows, approximately between 470 and 570 minutes, power injection from an energy shifting battery that is also installed at the site.

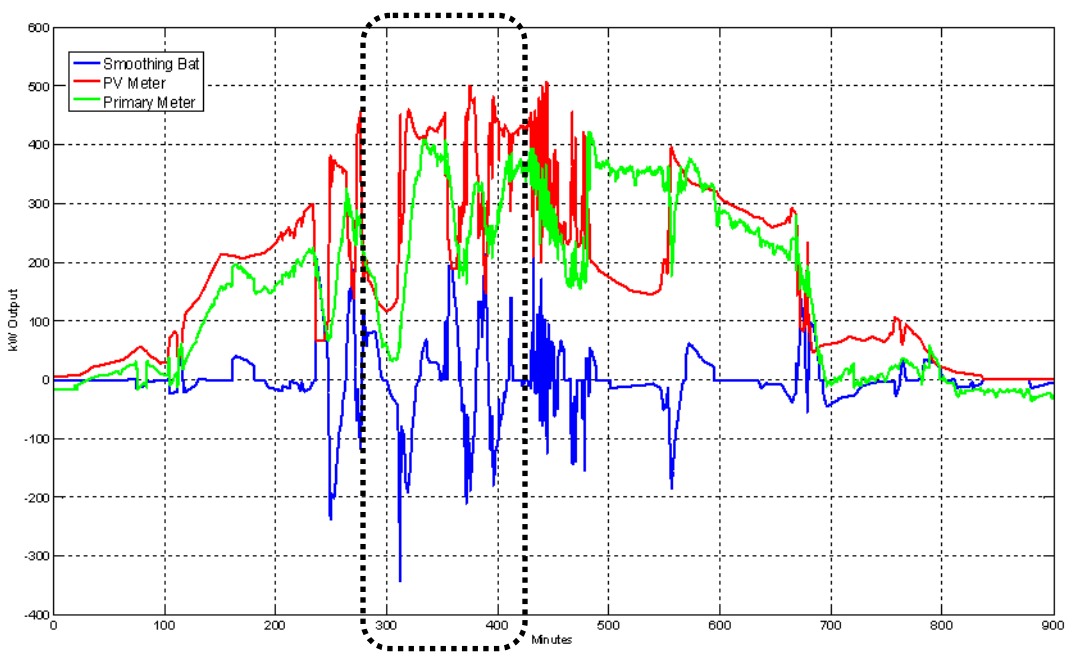

Fig 8. Power plots from demonstration site for a representative day

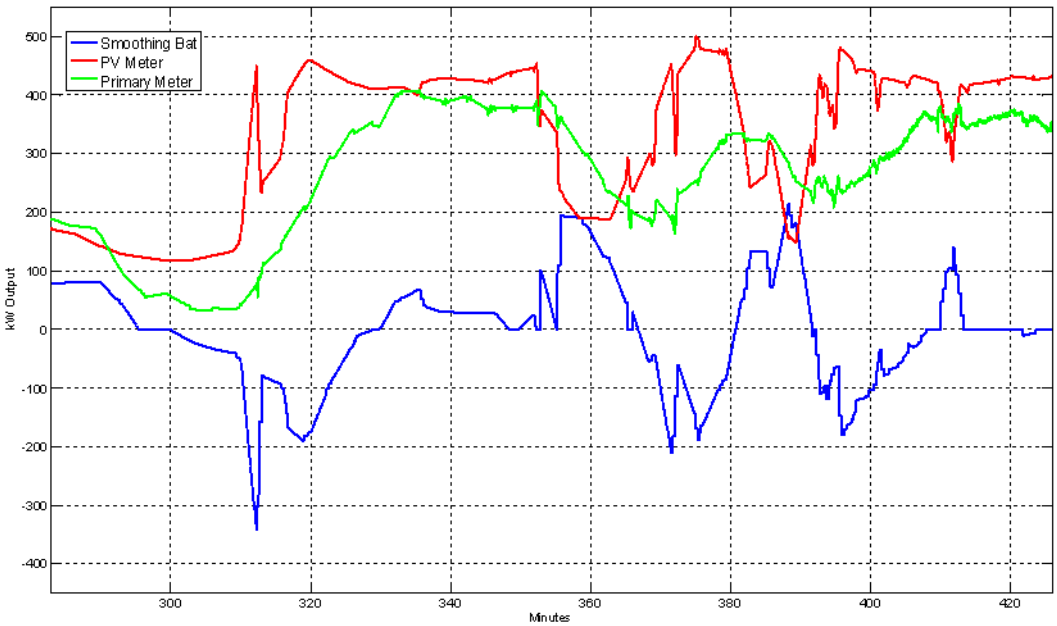

Fig 9. Detail of the dashed area in Fig. 8

While controls can be optimized by simulation, demonstration of stable and predictable performance in the field significantly increases operator confidence. Field demonstration also provided an opportunity to address challenging information integration issues required to achieve acceptable performance. The IT solution developed for this project is unique due to the need to support multiple protocols translation, handle data from a variety of sources and sampling rates, and the need to meet performance, reliability and security.

6. CONCLUSION

This paper describes an algorithm designed to reduce the variability of photovoltaic (PV) power output by using a battery. The algorithm presented was designed to be implemented in real time thus it does not contain a significant amount of complexity. The system parameters (battery capacity, rating of converters, and PV system rating) were assumed to be fixed. This exercise did not attempt to optimize the size of the energy storage system. Different battery parameter values would likely result in a change in the nominal parameter values needed to produce continued satisfactory overall performance.

A very simple model was used to represent the battery system. The effect of temperature, charge/discharge rate, efficiency and equalization charging were not considered. Such refinement could be added to the model, but their impact on the overall controller performance is not expected to be very significant. In this implementation, only MA and LPF smoothing options were evaluated. More sophisticated options with more general filtering capabilities are certainly possible, but were not evaluated. In addition, a few changes to the control system could be made to improve the robustness of the control system to battery parameters and time delays. The dead band function helps, but other changes could include variable gains that adapt depending on the magnitudes of the error signals or incorporating prediction functions to correct for time delays naturally introduced by the MA and LPF functions. Finally, more testing can be done to demonstrate the addition of the two auxiliary signals to show their effects on the algorithm's performance. As discussed in Sec. 5, the experimentation is ongoing as part of the field demonstration.

7. REFERENCES

1. O. Lavrova, F. Cheng, Sh. Abdollahy, A. Mammoli, S. Willard, B. Arellano, and C. van Zeyl, "Modeling of PV plus Storage for Public Service Company of New Mexico's Prosperity Energy Storage Project," 2011 Electrical Energy Storage Applications & Technologies Conference (EESAT), San Diego, CA, Oct. 16-19, 2011.
2. A. Ellis, D. Schoenwald, J. Hawkins, S. Willard, and B. Arellano, "PV Output Smoothing with Energy Storage," 38th IEEE Photovoltaic Specialists Conference, Austin, TX, June 3-8, 2012.
3. A. Ellis and D. Schoenwald, "PV Output Smoothing with Energy Storage," Sandia National Laboratories Technical Report, SAND2012-1772, March 2012.
4. T. Hund, S. Gonzalez, and K. Barrett, "Grid-Tied PV System Energy Smoothing,"35th IEEE Photovoltaics Specialists Conference (PVSC), Honolulu, HI, pp. 2762-2766, June 20-25, 2010.
5. H. Fakham, D. Lu, and B. Francois, "Power Control Design of a Battery Charger in a Hybrid Active PV Generator for Load-Following Applications," IEEE Transactions on Industrial Electronics, Vol. 58, No. 1, pp. 85-94, Jan. 2011.
6. T. Kinjo, T. Senjyu, N. Urasaki, and H. Fujita, "Output Levelling of Renewable Energy by Electric Double-Layer Capacitor Applied for Energy Storage System," IEEE Transactions on Energy Conversion, Vol. 21, No. 1, pp. 221-227, March 2006.

DISTRIBUTION

External distribution (*distributed electronically unless otherwise noted*):

1 Jon Hawkins (paper)
Public Service Company of New Mexico
414 Silver Avenue SW
Albuquerque, NM 87102-3289

1 Steve Willard (paper)
Public Service Company of New Mexico
414 Silver Avenue SW
Albuquerque, NM 87102-3289

1 Brian Arellano (paper)
Public Service Company of New Mexico
414 Silver Avenue SW
Albuquerque, NM 87102-3289

Internal distribution (*distributed electronically unless otherwise noted*):

1	MS1033	Abraham Ellis	06112 (paper)
1	MS1033	Charles J. Hanley	06112 (paper)
1	MS1104	Rush D. Robinett III	06110
1	MS1140	Raymond H. Byrne	06113
1	MS1140	Ross Guttromson	06113 (paper)
1	MS1140	David A. Schoenwald	06113 (paper)
1	MS0899	Technical Library	09536

Sandia National Laboratories